

Incoherent elastic and quasi-elastic neutron scattering investigation of hemoglobin dynamics

Chiara Caronna^{a,b}, Francesca Natali^{a,*}, Antonio Cupane^b

^aINFM OGG & CRS-SOFT, c/o ILL, 6 rue Jules Horowitz, BP 156-38042 Grenoble Cedex 9, France

^bIstituto Nazionale per la Fisica della Materia and Dipartimento di Scienze Fisiche ed Astronomiche, Università di Palermo, via Archirafi 36, I-9023, Palermo, Italy

Received 8 February 2005; accepted 17 February 2005

Available online 23 May 2005

Abstract

In this work we investigate the dynamic properties of hemoglobin in glycerolD₈/D₂O solution using incoherent elastic (ENS) and quasi-elastic (QENS) neutron scattering. Taking advantage of complementary energy resolutions of backscattering spectrometers at ILL (Grenoble), we explore motions in a large space–time window, up to 1 ns and 14 Å; moreover, in order to cover the harmonic and anharmonic protein dynamics regimes, the elastic experiments have been performed over the wide temperature interval of 20–300 K. To study the dependence of the measured dynamics upon the protein quaternary structure, both deoxyhemoglobin (in T quaternary conformation) and carbon-monoxymoglobin (in R quaternary conformation) have been investigated.

From the ENS data the mean square displacements of the non-exchangeable hydrogen atoms of the protein and their temperature dependence are obtained. In agreement with previous results on hydrated powders, a dynamical transition at about 220 K is detected. The results show interesting differences between the two hemoglobin quaternary conformations, the T-state protein appearing more rigid and performing faster motions than the R-state one; however, these differences involve motions occurring in the nanosecond time scale and are not detected when only faster atomic motions in the time scale up to 100 ps are investigated.

The QENS results put in evidence a relevant Lorentzian quasi-elastic contribution. Analysis of the dependence of the Elastic Incoherent Structure Factor (EISF) and of the Lorentzian halfwidth upon the momentum transfer suggests that the above quasi-elastic contribution arises from the diffusion inside a confined space, values of confinement radius and local diffusion coefficient being compatible with motions of hydrogen atoms of the amino acid side chains. When averaged over the whole range of momentum transfer the QENS data put in evidence differences between deoxy and carbonmonoxymoglobin and confirm the quaternary structure dependence of the protein dynamics in the nanosecond time scale.

© 2005 Elsevier B.V. All rights reserved.

Keywords: Protein dynamics; Hemoglobin quaternary structure; Mean square displacement; Dynamical transition

1. Introduction

It is nowadays generally accepted that proteins are dynamic objects and that the dynamic properties are relevant to protein functions. In particular, a variety of techniques (including, e.g., Mössbauer spectroscopy [1], neutron scattering [2], optical absorption spectroscopy [3]

and molecular dynamics simulations [4]) have shown a transition, occurring in the range 180–220 K, in the dynamic behavior of hydrated proteins from a low temperature harmonic behavior to an high temperature anharmonic behavior characterized by an increase of atomic mean square displacements well above the “harmonic” hyperbolic cotangent behavior. The onset of anharmonic dynamics has often been deemed necessary for optimal enzyme activity and protein function [5]. On the other hand, motions in proteins are known to exist in a wide range of time and length scales, spanning, e.g., from local atomic

* Corresponding author. Tel.: +33 4 76 20 70 71; fax: +33 4 76 48 39 06.

E-mail address: natali@ill.fr (F. Natali).

vibrations (10^{-12} s and 10^{-1} Å time and length scale) to concerted motions of protein segments (10^{-3} s and 10^1 Å). Therefore, when studying protein dynamics and in particular the transition between harmonic and anharmonic regimes, attention must be paid to the time and length scale probed by the experimental technique used. As an example, for the enzyme glutamate dehydrogenase the dynamical transition has been shown to be highly time scale dependent [6] and enzyme activity has been shown to be unaffected by anharmonic motions taking place in the picosecond time scale.

As far as hemoglobin is concerned, dynamic studies are further complicated by the possible presence of effects linked to the quaternary conformation. Indeed, it is well known that hemoglobin can reversibly adopt two different quaternary conformations: the tense (T) conformation, in the absence of ligands, and the relaxed (R) conformation, stabilized by the presence of ligands such as CO or O₂. The widely different structural and functional properties of the two conformations are well characterized [7,8]. Much less is known about their dynamic properties and about the structure–dynamics–function relationships of the two different quaternary conformations. Low temperature optical absorption spectroscopy has pointed out remarkable differences between the dynamic properties of deoxyhemoglobin (deoxyHb) and carbonmonoxyhemoglobin (HbCO) [9,10]. However, optical spectroscopy is an “instantaneous” technique that probes the local dynamic properties of the active site (i.e. of the heme pocket) which is highly dependent upon the local tertiary structure and in particular upon the presence/absence of the heme ligand. Therefore, information on the dependence of the global protein dynamics upon the time scale investigated and upon the quaternary conformation, as well as on the possible relevance of dynamic properties in determining the functional behavior of the molecule in different quaternary conformations is up to now lacking.

Incoherent neutron scattering from proteins in deuterated solutions, which is primarily sensitive to the non-exchangeable hydrogen atoms of the protein, appears as a technique suited to address the above points [11,12]. Indeed, being biomolecules made up mainly of H (around 50% of the total atom numbers), C, O and N atoms, the incoherent signal arises principally from the H atoms whose incoherent cross section is two orders of magnitudes higher than that of the remaining atoms; moreover, non-exchangeable hydrogen atoms are evenly distributed over the whole protein. On the other hand, the solvent contributions can be subtracted by performing accurate scans on a “blank” sample, i.e. on a sample containing identical quantities of solvent, buffer and salts and in which only the protein is missing. Thus, the incoherent neutron scattering technique (INS), which describes the correlation of a given particle at different times, provides information on the global molecule dynamics. Moreover, by exploiting the different energy resolutions and momentum transfer (Q) ranges of different spectrom-

eters, motions occurring in different time and length scales can be investigated.

In this paper we present the results of an incoherent elastic and quasi-elastic neutron scattering investigation of hemoglobin dynamics. Experiments have been performed on 65% glycerolD₈/D₂O solutions of both deoxyHb and HbCO; the presence of glycerolD₈ as a cryosolvent is necessary in order to span a wide temperature range, covering the harmonic and anharmonic regimes, without the appearance of undesired ice Bragg reflections. Two different spectrometers at ILL (Grenoble) have been used: IN13 with an energy resolution of ~ 8 μ eV (FWHM) and a Q range of ~ 1.1 – 5.0 Å⁻¹ and IN16 with an energy resolution of ~ 0.9 μ eV (FWHM) and a Q range of ~ 0.4 – 1.9 Å⁻¹. This enables to explore motions occurring in the time scale up to 100 ps and 1 ns, respectively, and in the length scale from ~ 1 Å to ~ 14 Å. Aim of the work is to investigate the dynamic properties of hemoglobin in solution in the widest possible time and length intervals and to put in evidence the possible presence of effects linked to the quaternary structure of the protein.

2. Materials and methods

2.1. Samples

Hemoglobin was prepared from the blood of a single healthy individual as already described elsewhere [13]; it was stored in liquid nitrogen under the oxy form at a concentration of about 10% by weight. To prepare samples for the experiments, an appropriate amount was thawed and deuterated by first concentrating to about 30% by weight and then re-diluting to 10% with D₂O (Euro-isotope, Grenoble, France, purity >99.8%). This procedure was repeated several times, to reach a final D₂O/H₂O concentration greater than 98:1. Samples were then mixed with glycerolD₈ (Euro-isotope, Grenoble, France, purity >99.8%) in a 1:2 proportion and with phosphate buffer 1 M (pD=7) to have a final buffer concentration of 10^{-2} M. Use of glycerolD₈ as a cryoprotectant allows us to expand the explored temperature range towards low T values ($T < 273$ K), normally limited by the presence of ice Bragg reflections.

To prepare deoxy Hb, the sample was equilibrated with N₂ by gently stirring under nitrogen atmosphere for about 15 min and then deoxygenated with 5×10^{-2} M sodium dithionite. To prepare HbCO, exactly the same procedure was followed, using CO as equilibration gas.

The pD of the samples was measured immediately after preparation and found to be around 6.7 for both samples.

2.2. Neutron scattering experiments

Neutron scattering experiments have been performed on two high-resolution backscattering spectrometers, which

allow us to extend the time scale accessible. Hereon, we will denote with fast and slow scales motion the dynamics explored with lower (IN13) and higher (IN16) instrument energy resolutions, respectively.

For the elastic investigation of the fast atomic motion, incoherent elastic neutron scattering temperature scans were performed on the thermal ($\lambda=2.23$ Å) backscattering spectrometer IN13 (ILL) that allows to access to the already cited high momentum transfers (Q) with a good and almost Q -independent energy resolution. IN13, therefore, spans the space and time windows of 1–6 Å and 0.1 ns, respectively, providing detailed information on the motion of the H atoms present in the sample [14]. The beam scattered from the sample was reflected in almost perfect backscattering geometry by CaF_2 analysers to be finally collected by 32 He^3 detectors. The elastic energy value ($\hbar\omega=0$) was kept fixed within 3 μeV of accepted tolerance. The elastic scattering intensities ($I_{\text{el}} \equiv S(Q, \omega=0)$) were corrected for solvent and cell contributions by performing a temperature scan on a “blank” sample, i.e. on a sample containing identical quantities of D_2O , glycerol D_8 , buffer and dithionite and in which only the protein was missing. They were also normalized with respect to the lowest temperature scan ($T=20$ K) to compensate for spurious background contributions and detector efficiency.

For the elastic and quasi-elastic investigations of the slow atomic motion, spectra have been acquired using the high-energy resolution backscattering spectrometer IN16 (ILL). It provides information in the 3.5–14.5 Å and 1 ns space–time window [15]. The quasi-elastic scattering intensities were corrected for solvent and cell contributions, and normalized with respect to a standard totally incoherent sample (Vanadium), used as detector calibration.

For both IN13 and IN16 elastic scans, the temperature was varied from 20 to 300 K, while IN16 quasi-elastic spectra have been measured at room temperature. In order to avoid correction from multiple scattering contribution, in all the experiments here described, the sample thickness was properly chosen to minimize the neutron absorption from the sample. A typical transmission percentage of 90% was guaranteed using 1 mm thick Al flat sample holder.

3. Results

3.1. Elastic scans

The normalized incoherent elastic scattering function $S(Q, \omega=0)$ vs. the squared momentum transfer was measured as a function of temperature.

The data have been analyzed in terms of the Gaussian model valid in the Q range where $\sqrt{\langle \Delta u^2 \rangle Q^2 / 2} \leq 1$ [16]. In this context the elastic scattering intensity $I(Q, \omega=0)$ is given by:

$$I(Q, \omega=0) = I_0 e^{-\frac{\langle \Delta u^2 \rangle}{6} Q^2} \quad (1)$$

where $\langle \Delta u^2 \rangle = \langle u_{\text{tot}}^2(T) \rangle - \langle u_{\text{tot}}^2(20 \text{ K}) \rangle$ is the total mean square displacement (MSD) of non-exchangeable hydrogen atoms of the protein. $\langle \Delta u^2 \rangle_{\text{tot}}$ is obtained by fitting the experimental data with Eq. (1) in the Q^2 range 1.21–4.84 Å $^{-2}$ for the IN13 experiment and 0.2–1.2 Å $^{-2}$ for the IN16 experiment. In Fig. 1 are reported the fits of typical IN16 data at selected temperatures; filled symbols refer to deoxyHb, empty symbols to HbCO. The temperature dependence of $\langle \Delta u^2 \rangle_{\text{tot}}$ for both samples is reported in Fig. 2; panels a and b refer to the IN13 and IN16 experiments, respectively.

Some relevant facts are evident from inspection of the data reported in Fig. 2:

- The temperature dependence of $\langle \Delta u^2 \rangle_{\text{tot}}$ is characterized by the well known broad “dynamical” transition at about 220 K which has been observed for many proteins using a variety of spectroscopic techniques [1,2,17–21]. However, while $\langle \Delta u^2 \rangle_{\text{tot}}$ values measured with IN13 and IN16 agree at low temperatures, a difference is present at $T > 250$ K, where $\langle \Delta u^2 \rangle_{\text{tot}}$ values measured with IN16 are remarkably larger than those measured with IN13. This is not surprising, in our opinion, in view of the ampler space and time domain investigated with IN16 with respect to IN13. The different Q range accessible with the two spectrometers may be particularly relevant also in the application of the Gaussian approximation. The dependence of obtained $\langle \Delta u^2 \rangle_{\text{tot}}$ values upon the spatial and temporal resolution of the experiment has been thoroughly discussed in [6,16].
- Protein motions seem not to be environment dependent up to 260 K, as suggested by the comparison of our data with those obtained on MetHb hydrated powders as measured by Tengroth et al. on the IRIS

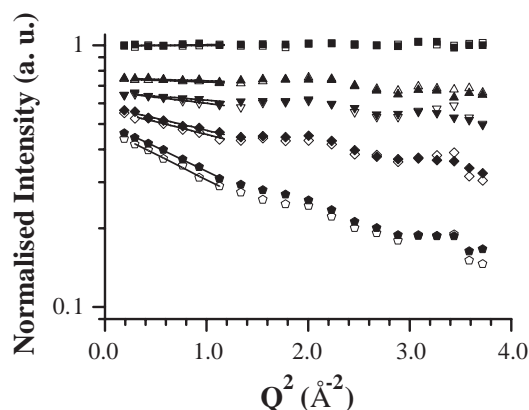


Fig. 1. Temperature dependence of the normalized elastic scattering function $S(Q, \omega=0)$ vs. Q^2 , as measured on IN16. Squares: $T=35$ K; triangles up: $T=225$ K; triangles down: $T=255$ K; rhombs: $T=275$ K; pentagons: $T=300$ K. Filled symbols: deoxyHb; empty symbols: HbCO. The lines represent fits of the experimental data in the Q^2 range 0.2–1.2 Å $^{-2}$ using Eq. (1) in the text.

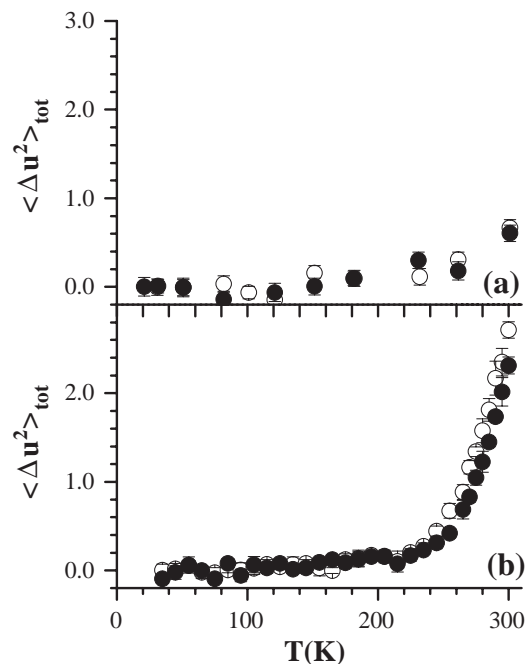


Fig. 2. Hydrogen atoms MSD as measured on IN13 (panel a) and IN16 (panel b). Filled symbols: deoxyHb; empty symbols: HbCO.

spectrometer (ISIS, UK) [22]. Comparison of the behaviour of the two systems at higher temperatures is not possible, being the IRIS data not yet published.

- (c) As far as the IN13 data are concerned, even though the data suffer from somewhat low statistics, no systematic differences between deoxyHb and HbCO can be observed up to room temperature. This would imply that the fast motions of hemoglobin (i.e. motions occurring in a $t \sim 100$ ps time scale) are not influenced by the quaternary conformation of the protein. On the contrary, by looking at the IN16 data a small but systematic difference between the two samples appears at $T > 250$ K; in particular, $\langle \Delta u^2 \rangle_{\text{tot}}$ values relative to deoxyHb are systematically lower by about 15% than those relative to HbCO and the “dynamical transition” temperature is higher (~ 230 K for deoxyHb as compared to ~ 210 K for HbCO). This relevant result would imply that when hemoglobin dynamics is observed on ampler time and length scale (up to ~ 1 ns and ~ 14 Å) it appears influenced by the quaternary conformation of the protein and in particular deoxyHb (in T quaternary conformation) appears characterized by smaller MSD values with respect to HbCO (in R quaternary conformation).

3.2. Quasi-elastic scans

To obtain more detailed information on the dynamics, we performed quasi-elastic scans on IN16 for both samples at room temperature. In Fig. 3 we report the normalized room

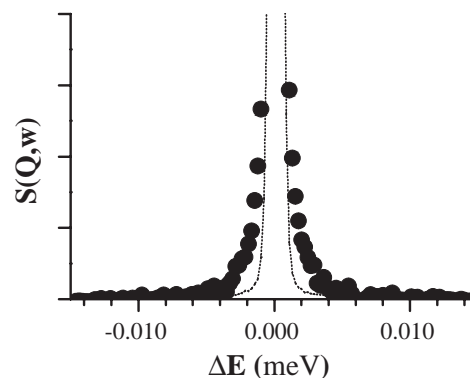


Fig. 3. Filled symbols: normalized room temperature QENS spectrum of HbCO measured on IN16, binned over the whole Q range accessible. Dotted line: instrument resolution.

temperature QENS spectrum of HbCO, binned over the whole Q range accessible and plotted together with the instrument resolution. A relevant QENS contribution is clearly observed.

Semi-quantitative information on the dynamics of the system and on differences between HbCO and deoxyHb can be obtained by analyzing the Q -binned data; this approach is necessary to reach the required statistical data accuracy. Within this “zero order” approach the Q -averaged incoherent quasi-elastic neutron scattering structure function can be written, using standard notations, as:

$$\langle S(Q, \omega) \rangle_Q = \langle e^{-\frac{(\Delta u^2)}{6} Q^2} \rangle_Q [A_0 \delta(\omega) + (1 - A_0) L(\omega)] R(\omega) + C \quad (2)$$

where A_0 is the Elastic Incoherent Structure Factor (EISF), $L(\omega)$ is the quasi-elastic component (assumed to have

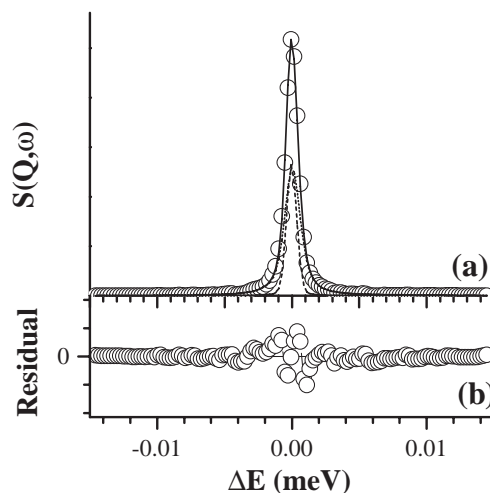


Fig. 4. Panel a: Fit of the HbCO experimental data, binned over the whole Q range accessible, in terms of Eq. (2). Panel b: Residuals reported on an expanded scale. Empty symbols: experiment; continuous line: fit; dashed line: elastic peak; dotted line: quasi-elastic peak.

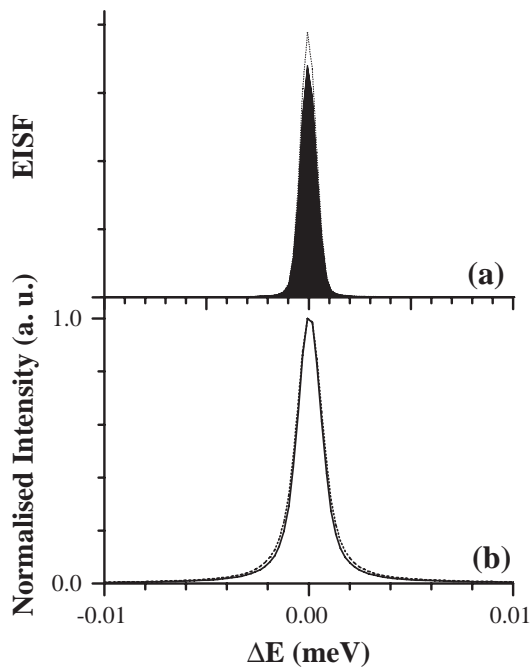


Fig. 5. Elastic (panel a) and quasi-elastic (panel b) contributions for both deoxyHb and HbCO samples, as obtained from the fits of experimental data with Eq. (2). Dotted line: Hb-deoxy; continuous line: HbCO.

Lorentzian shape) and $R(\omega)$ is the experimental resolution function. A flat background (the C term in Eq. (2)) is also added, to take into account inelastic contributions in the QENS energy region. As mentioned in the Materials and methods, the instrument resolution is measured using a totally incoherent sample, a vanadium plate of 1 mm thickness, which is normally considered as the instrument calibration scan; it is also binned over the entire Q range. Very good agreement between experiment and theory is obtained for all the data set, as exemplified in Fig. 4. The normalized elastic and quasi-elastic contributions relative to both samples, as obtained from fits in terms of Eq. (2), are reported in Fig. 5, while values of parameters A_0 and Γ (HWHM) of the quasi-elastic Lorentzian contribution are reported in Table 1.

Significative differences between HbCO and deoxyHb are evident in Fig. 5 and Table 1; in particular for deoxyHb the Q -integrated EISF and Γ values are larger by $\sim 7\%$ and $\sim 14\%$, respectively. This suggests more localised diffusive-like motions for deoxyHb (in T conformation) occurring in a shorter time scale, and is in agreement with the smaller MSD value evidenced at this temperature by the elastic scans.

Table 1
Values of physical parameters obtained from the fits on Q -averaged data

| | EISF | Γ (μeV) |
|---------|------|-----------------------------|
| HbCO | 0.40 | 0.58 |
| deoxyHb | 0.43 | 0.66 |

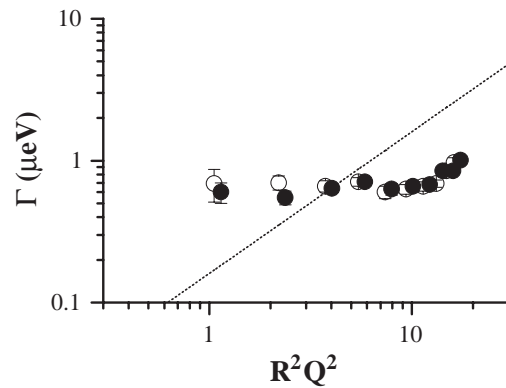


Fig. 6. Γ (HWHM) of the Lorentzian line as a function of R^2Q^2 , for both samples; R is the radius of the confinement sphere (see Table 2). Filled symbols: deoxyHb; empty symbols: HbCO. The line represents the asymptotic behaviour predicted by the Fick's law.

More detailed information on the type of motions involved in the measured quasi-elastic contribution requires the study of the Q dependence of the Lorentzian broadening Γ and of the EISF. For this type of analysis we used the following expression:

$$S(Q, \omega) = \exp\left(-\frac{\langle \Delta u^2 \rangle}{6} Q^2\right) [A_0(Q)\delta(\omega) + (1 - A_0(Q))L(Q, \omega)]R(Q, \omega) + C(Q) \quad (3)$$

Eq. (3) is substantially equivalent to Eq. (2), the only difference being that the various physical quantities (EISF, Lorentzian quasi-elastic component and the experimental resolution function) are now dependent upon the momentum transfer Q . In order to gain in signal to noise ratio, the data have been binned over two consecutive Q values; the Q dependence of the Lorentzian broadening Γ and of EISF is reported in Figs. 6 and 7, respectively.

It is evident from Fig. 6 that the data do not show a Fick-type behaviour ($\Gamma(Q) = D \times Q^2$) in the low- Q limit but extrapolate to a non-zero value; in fact the QENS broadening exhibits a constant regime up to $Q \leq 1.5 \text{ \AA}^{-1}$, followed by an increase at higher Q values. This behaviour

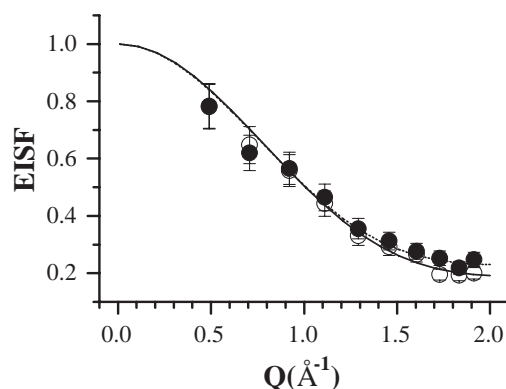


Fig. 7. EISF as a function of Q for both samples. Filled symbols: deoxyHb; empty symbols: HbCO. Lines are fits according to Eq. (5).

is compatible with the absence of long-range diffusive motions in our samples and suggests the presence of diffusion within a confined volume, such as the diffusion within a sphere [23]. It should also be noted that with this type of analysis the statistical accuracy of the data is not sufficient to detect differences in the Q dependence of Lorentzian broadening of deoxyHb and HbCO.

On the other hand, EISF values reported in Fig. 7 clearly show a tendency to an asymptotic non-zero value (close to 0.2) in the high Q region. This behaviour has been observed in previous QENS experiments on proteins [24] and can be reconciled with restricted diffusion models by hypothesizing that some of the hydrogens contributing to the spectrum perform only vibrational harmonic motions and therefore appear as “fixed”.

As already reported in the literature [24], it is then possible to separate the total EISF into two contributions:

$$\text{EISF}_E = A_0(Q) = f \cdot \text{EISF}_F + (1 - f) \cdot \text{EISF}_M \quad (4)$$

where EISF_E is the experimental EISF (Fig. 7), f is fraction of fixed protons (within the IN16 time window), EISF_F and EISF_M represent the values associated to the fixed and mobile protons, respectively. By definition of fixed protons, $\text{EISF}_F = 1$; Eq. (4) then reduces to:

$$\text{EISF}_E = f + (1 - f) \cdot \text{EISF}_M \quad (5)$$

Modelling the motion of the mobile hydrogens as a restricted diffusion within a sphere one has [23]:

$$\text{EISF}_M(Q) = \left[\frac{3J_1(QR)}{QR} \right]^2 \quad (6)$$

where $J_1(QR)$ is the first order spherical Bessel function and R is the radius of the confinement sphere. The lines in Fig. 7 represent fits of the experimental data in terms of the model (Eqs. (4)–(6)); values of physical quantities obtained from the above analysis are reported in Table 2.

Values of parameter f relative to HbCO and deoxyHb show a small, but not negligible difference: $f_{\text{HbCO}} = 0.19$ while $f_{\text{Hb-deoxy}} = 0.23$, in agreement with the results obtained from the Q -averaged analysis (Fig. 5), suggesting once again a more rigid conformation (i.e. more “fixed” protons) for deoxyHb. On the other hand, R values around 2.2 Å are compatible with the assignment of the mobile protons to hydrogen atoms of the amino acid side chains.¹

¹ Further confirmation of the analysis performed has been obtained by taking advantage of a model dependent data analysis program, named AGATHE (Application for General Analysis of Time-of-flight and High resolution Experiment) (courtesy of Prof. M. Bée). The approach forces the experimental data in all the Q -range available to be fitted with common D and R values, as obtained from the theoretical model (in our case the “restricted diffusion inside a sphere” model by Volino and Dianoux, [23]) while in the free-model analysis the determination of these parameters is provided a posteriori and the fit is free of any constraints. Using the AGATHE program, optimal agreement between experimental and theoretical data has been obtained.

Table 2

Values of physical parameters obtained by fitting the data in terms of the Q -dependent model (Eqs. (4)–(6) in the text)

| | f | R (Å) | D ($\mu\text{eV}\cdot\text{\AA}^2$) |
|---------|-----------------|-----------------|---|
| HbCO | 0.19 ± 0.01 | 2.10 ± 0.07 | 0.7 ± 0.1 |
| DeoxyHb | 0.23 ± 0.01 | 2.18 ± 0.08 | 0.7 ± 0.1 |

f represents the fraction of immobile protons, R the radius of the confinement sphere and D the local diffusion coefficient, obtained from the data in Fig. 6 according to $\Gamma(Q \rightarrow 0) = 4.33D/R^2$ [25].

Further insight may be obtained by comparing our results with the QENS data on metHb hydrated powders (IRIS, ISIS-UK) reported by Tengroth et al. [22]. These authors report the presence of a relevant QENS contributions at temperatures higher than ~ 220 K. However, the halfwidth of the quasi-elastic Lorentzian line is, in their case, about 7.5 μeV , as compared to our value of about 0.5 μeV ; moreover, given the energy interval spanned in our IN16 quasi-elastic scan (-15 μeV , $+15$ μeV), the quasi-elastic Lorentzian line observed by Tengroth et al. [22] contributes, in our experiment, only as a flat background (the constant term C in Eqs. (2) and (3)); conversely, given the Tengroth et al. [22] experimental resolution (HWHM 7.5 μeV), our quasi-elastic Lorentzian line falls completely within the elastic peak in the IRIS data. All this suggests that different motions are being observed in the two experiments.

4. Conclusion

In this work the dynamics of hemoglobin in 65% glycerolD₈/D₂O solution and its dependence upon the quaternary structure of the protein has been investigated with incoherent elastic and quasi-elastic neutron scattering. The main results of the work can be summarized as follows:

- (1) The MSD of non-exchangeable hydrogen atoms of the protein have been determined through elastic scans in the temperature interval 20–300 K. In agreement with previous results in the literature [22] on met-hemoglobin hydrated powders, a so-called “dynamical transition” is observed at temperatures around 220 K from a low temperature harmonic behavior to a high temperature non-harmonic behavior; this is usually attributed to the onset of new conformational degrees of freedom connected to the jump between different conformational substates of the protein [26]. Our data put in evidence the dependence of the thermal behavior of MSD on the time and length scale investigated. Concerning the dependence of hydrogen atoms MSD from the protein quaternary structure, while no effect is measured on IN13, a small but systematic difference is observed on IN16. Indeed, for deoxyHb (in T quaternary conformation) the MSD values above the dynamical transition are found about

15% smaller than for HbCO. This result suggests that the hemoglobin quaternary structure does not influence protein motions occurring in the time scale up to 100 ps, while it is effective in affecting motions occurring in the nanosecond time regime. When examined in the time and length scales larger than 100 ps and 5 Å, respectively, hemoglobin in T conformation appears more rigid than hemoglobin in R conformation.

- (2) The type of motions involved has been investigated with quasi-elastic runs performed on IN16 at room temperature. The results show the presence of a relevant quasi-elastic Lorentzian contribution. When the data are averaged over all Q values to increase their statistical relevance, a larger EISF and a broader Lorentzian halfwidth are found for deoxyHb with respect to HbCO, the effect being on the order of 10%. This confirms the elastic results and suggests that Hb in T conformation is more rigid and performs faster motions than Hb in R conformation. The Q dependence of EISF and Lorentzian width can be analyzed using the “restricted diffusion inside a sphere” model of Volino and Dianoux [23]; in this way a confinement radius of about 2.2 Å and a local diffusion coefficient of $0.7 \mu\text{eV}\cdot\text{\AA}^2$ are found, compatible with motions of hydrogen atoms of amino acid side chains. Moreover, from the Q -dependent analysis a larger number of “fixed” protons is evidenced for deoxyHb, confirming an increased rigidity of Hb in T quaternary conformation in agreement with elastic and Q -binned quasi-elastic results.

References

- [1] F.G. Parak, Physical aspects of protein dynamics, *Rep. Prog. Phys.* 66 (2003) 103–129.
- [2] W. Doster, S. Cusack, W. Petry, Dynamical transition of myoglobin revealed by inelastic neutron scattering, *Nature* 337 (1989) 754–756.
- [3] B. Melchers, E.W. Knapp, F. Parak, L. Cordone, A. Cupane, M. Leone, Structural fluctuations of myoglobin from normal-modes. Mössbauer, Raman and absorption spectroscopy, *Biophys. J.* 70 (1996) 2092–2096.
- [4] P.J. Steinbach, R.J. Loncharich, B.R. Brooks, The effects of environment and hydration on protein dynamics: a simulation study of myoglobin, *Chem. Phys.* 158 (1991) 383–394.
- [5] R.M. Daniel, J.C. Smith, M. Ferrand, S. Hery, R. Dunn, J.L. Finney, Enzyme activity below the dynamical transition at 220 K, *Biophys. J.* 75 (1998) 2504–2507.
- [6] R.M. Daniel, J.L. Finney, V. Réat, R. Dunn, M. Ferr, J.C. Smith, Enzyme dynamics and activity: time scale dependence of dynamical transitions in Glutamate Dehydrogenase solution, *Biophys. J.* 77 (1999) 2184–2190.
- [7] M.F. Perutz, A.J. Wilkinson, M. Paoli, G.G. Dodson, The stereochemical mechanism of the cooperative effects in hemoglobin revisited, *Annu. Rev. Biophys. Biomol. Struct.* 27 (1998) 1–34.
- [8] R.E. Dickerson, I. Geis, Hemoglobin, Benjamin Cummings, Menlo Park, USA, 1983.
- [9] A. Cupane, M. Leone, E. Vitrano, Protein dynamics: conformational disorder, vibrational coupling and anharmonicity in deoxyhemoglobin and myoglobin, *Eur. Biophys. J.* 21 (1993) 385–391.
- [10] A. Cupane, M. Leone, E. Vitrano, L. Cordone, Low temperature optical absorption spectroscopy: an approach to the study of stereodynamic properties of heme proteins, *Eur. Biophys. J.* 23 (1995) 385–398.
- [11] F. Gabel, D. Bicout, U. Lehnert, M. Tehei, M. Weik, G. Zaccai, Protein dynamics studied by neutron scattering, *Q. Rev. Biophys.* 35 (2002) 327–367.
- [12] G. Zaccai, How soft is a protein? A protein dynamics force constant measured by neutron scattering, *Science* 288 (2000) 1604–1607.
- [13] L. Cordone, A. Cupane, P.L. San Biagio, E. Vitrano, Effect of some monohydric alcohols on the oxygen affinity of hemoglobin: relevance of solvent dielectric constant and hydrophobicity, *Biopolymers* 18 (1979) 1975–1988.
- [14] IN13 Yellow Book, <http://www.ill.fr/YellowBook/IN13/>.
- [15] IN16 Yellow Book, <http://www.ill.fr/YellowBook/IN16/>.
- [16] T. Becker, J.C. Smith, Energy resolution and dynamical heterogeneity effects on elastic incoherent neutron scattering from molecular systems, *Phys. Rev., E* 67 (2003) (021904-1-8).
- [17] M. Ferrand, A.J. Dianoux, W. Petry, J. Zaccai, Thermal motions and function of bacteriorhodopsin in purple membranes—effects of temperature and hydration studied by neutron scattering, *Proc. Natl. Acad. Sci. U. S. A.* 20 (1993) 9668–9672.
- [18] C. Andreani, A. Filabozzi, F. Menzinger, A. Desideri, A. Deriu, D. Di Cola, Dynamics of hydrogen atoms in superoxide dismutase by quasi-elastic neutron scattering, *Biophys. J.* 68 (1995) 2519–2523.
- [19] J. Fitter, The temperature dependence of internal molecular motions in hydrated and dry α -amylase: the role of hydration water in the dynamical transition of proteins, *Biophys. J.* 72 (1999) 1034–1042.
- [20] V. Réat, H. Patzelt, M. Ferrand, C. Pfister, D. Oesterhelt, G. Zaccai, Dynamics of different functional parts of bacteriorhodopsin: H-D labelling and neutron scattering, *Proc. Natl. Acad. Sci. U. S. A.* 95 (1998) 4970–4975.
- [21] A. Paciaroni, S. Cinelli, G. Onori, Effect of environment on the protein dynamical transition: a neutron scattering study, *Biophys. J.* 83 (2002) 1157–1164.
- [22] C. Tengroth, L. Börjesson, W.W. Kagunya, H.D. Middendorff, Dynamics of haemoglobin through the 200 K glass-like transition, *Physica B* 266 (1999) 27–34.
- [23] F. Volino, A.J. Dianoux, Neutron incoherent scattering law for diffusion in a potential of spherical symmetry: general formalism and application to diffusion inside a sphere, *Mol. Phys.* 41 (1980) 271–279.
- [24] U.N. Wanderlingh, R. Giordano, A.J. Dianoux, F. Wanderlingh, IQENS dynamics in hydrated crambin, *Physica, A* 304 (2002) 276–282.
- [25] M.C. Bellissent-Funel, S.H. Chen, J.M. Zanotti, Single particle dynamics of water in a confined space, *Phys. Rev., E* 51 (1995) 4558–4569.
- [26] H. Frauenfelder, F. Parak, R.D. Young, Conformational substates in proteins, *Annu. Rev. Biophys. Biophys. Chem.* 17 (1988) 451–459.